Received: 14 January 2021 | Revised: 22 June 2022 | Accepted: 16 August 2022

DOI: 10.1111/pan.14545

Pediatric Anesthesia WILEY

RESEARCH REPORT

Magnetic resonance imaging study of the sciatic nerve variation in the pediatric gluteal region: Implications for the posterior approach of the sciatic nerve blockade

Sarang Byun[1] | Sarah Morris[2] | Nalini Pather[1]

[1]Department of Anatomy, School of Medical Sciences, Medicine and Health, UNSW Sydney, Sydney, New South Wales, Australia

[2]Department of Medical Imaging, Sydney Children's Hospital, Randwick, New South Wales, Australia

Correspondence
Sarang Byun, Department of Anatomy, School of Medical Sciences, Medicine and Health, UNSW Sydney, NSW 2052, Australia.
Email: christina.byun@unsw.edu.au

Section Editor: David M Polaner

Abstract

Introduction: In pediatric patients, the sciatic nerve is one of the most commonly blocked peripheral nerves during orthopedic procedures of the lower limb. Ultrasound guidance is the current standard for a successful localization of the sciatic nerve in the gluteal region. Relevant anatomical landmarks are also used to determine the nerve location when ultrasound is not available or inadequate. However, reports have demonstrated paucity of information regarding the sciatic nerve location and variation in the hip throughout pediatric development. This imaging study aimed to document and analyze the relative morphometric relationship of the sciatic nerve in the pediatric gluteal region throughout development.

Methods: The location of the sciatic nerve in relation to bony landmarks was measured in 84 pediatric magnetic resonance imaging of patients aged 0.7–15.8 years.

Results: The sciatic nerve was identified medial to the most lateral point of greater trochanter at the level of ischial spine and the tip of coccyx. The strong positive correlation between sciatic nerve to landmark distances and age and stature demonstrated linear variation between sciatic nerve location with age and growth of children. To predict the nerve location in the gluteal region, regression equations using patient age were created, having implications for the posterior approach of the sciatic nerve blockade in children. Clinically significant differences were found between sexes, specifically in the older age group.

Conclusion: Despite the small sample size of younger age group, this study is the first to document the morphometric changes of the sciatic nerve in the gluteal region across pediatric development and may be useful for providing confirmatory guidelines for nerve location when ultrasound is not accessible or cannot be utilized for practice.

KEYWORDS
anatomy, child, hip, magnetic resonance imaging, sciatic nerve

1 | INTRODUCTION

In the pediatric lower limb, the sciatic nerve is one of the most commonly blocked peripheral nerve for the management of pain after major orthopedic and surgical procedures to the leg, ankle, and foot.[1–3] Out of the three anterior, lateral, and posterior approaches of the sciatic nerve blockade in the gluteal region, the posterior approach has been recommended for its technical ease and effectiveness.[4–7] As illustrated in Figure 1, both adult[5,6,8–10] and pediatric[1,4,8,11,12] studies have reported needle insertion sites identified using the relevant anatomical landmarks for the posterior approach of the sciatic nerve blockade. In 2015, a computed tomography (CT) study was conducted to corroborate the location of the sciatic nerve relative to its surface landmarks in the adult gluteal region and provided a new revised description of the sciatic nerve landmarks.[10] Differing from traditional descriptions, the sciatic nerve was located significantly higher within the gluteal region. For the pediatric population, three clinical imaging studies have investigated the sciatic nerve location within the popliteal fossa, providing age-specific formulae for the popliteal approach of the sciatic nerve blockade.[2,13,14] No study to date, however, has investigated the morphometric relationship and location of the sciatic nerve within the gluteal region relative to age.

In the recent years, clinical studies have explored the course of the sciatic nerve in the gluteal region using ultrasonography,[15] developing ultrasound-guided techniques for the pediatric subgluteal approach of the sciatic nerve blockade.[16–18] Ultrasonography allows real-time visualization of the anatomical structures, location of the needle, and the spread of the local anesthetic, and has led to enhanced success rates of regional blockades.[7,15,17–19] In resource limited environments, however, there may be limits to employing ultrasound guidance due to the lack of available equipment and training and the prevalence of appropriate expertise.[2,20] The scalability of more developed techniques requires increased training and adoption by the clinicians,[21,22] especially for regional anesthetic practice where most training guidelines are still adult-oriented.[19]

Hence, this retrospective magnetic resonance imaging (MRI) study aimed to document and analyze the morphometric relationship of the sciatic nerve to the surrounding anatomical landmarks in the gluteal region across pediatric development. Through analyzing the quantitative data, this study aimed to determine whether correlations exist between age and the sciatic nerve location, and to provide age-specific guidelines for the identification of the sciatic nerve in the gluteal region, where landmark approaches need to be used in practice.

What is already known

- For a successful sciatic nerve blockade in the gluteal region, correct identification of the nerve is essential.
- Without ultrasound, landmark approaches are needed but there is paucity of information and inconsistencies in description of landmarks associated with the sciatic nerve location in the hip throughout pediatric development.

What this article adds

- This is the first clinical imaging study to verify the age-specific relations, location, and course of the sciatic nerve in the pediatric gluteal region.
- The age-related regression equation will have implications for needle placement in the posterior approach of the sciatic nerve blockade in children, where imaging equipment and expertise may not be adequate or available.

2 | MATERIALS AND METHODS

2.1 | Data collection

MRI scans of the pediatric hip region were obtained from the Sydney Children's Hospital following ethical approval (LNR/16/SCHN/387). An imaging dataset consisting of 132 de-identified MRI scans taken between December 2005 and April 2017 were exported in DICOM format for analysis using RadiAnt DICOM Viewer (version 5.0.2; Medixant). The exclusion criteria included MRI scans with poor resolution (e.g., from movement, variation in posture, and fat-suppressed scans), presence of pathology (e.g., soft tissue tumor), and/or the absence of the axial image plane. Following the exclusion criteria, a total of 84 scans (42 male and 42 female; 28 right side and 56 left side) were used in this study and the sample was grouped into three age categories (0–5, 6–11 and 12–16 years), as in the previous retrospective imaging study that determined the location of the sciatic nerve within the popliteal fossa.[14] For the 0–5 years age group (n = 17), the mean age was 3.7 ± 1.5 years (range 0.7–5.8), for the 6–11 years age group (n = 34), the mean age was 8.5 ± 1.4 years (range 6.2–11.0), and for the 12–16 years age group (n = 33), the mean age was 13.7 ± 1.6 years (range 11.1–15.8). The clinical data collected included patient information (sex and age), type of scan, region of scan, the limb side the measurements were taken from (i.e., right or left) and the scan thickness (in mm).

2.2 | Morphometric Measurements

Similar to the methodology for pediatric knee previously published,[14] morphometric measurements were taken of the sciatic nerve relative to neighboring anatomical landmarks (Figure 2). The morphometric parameters were measured at multiple levels (A–F) throughout the pediatric hip. The horizontal and diagonal width of the femur from the head to the most lateral point of the greater trochanter, at the level of the ischial spine (reference level D), were specifically measured as a control for variation in stature.

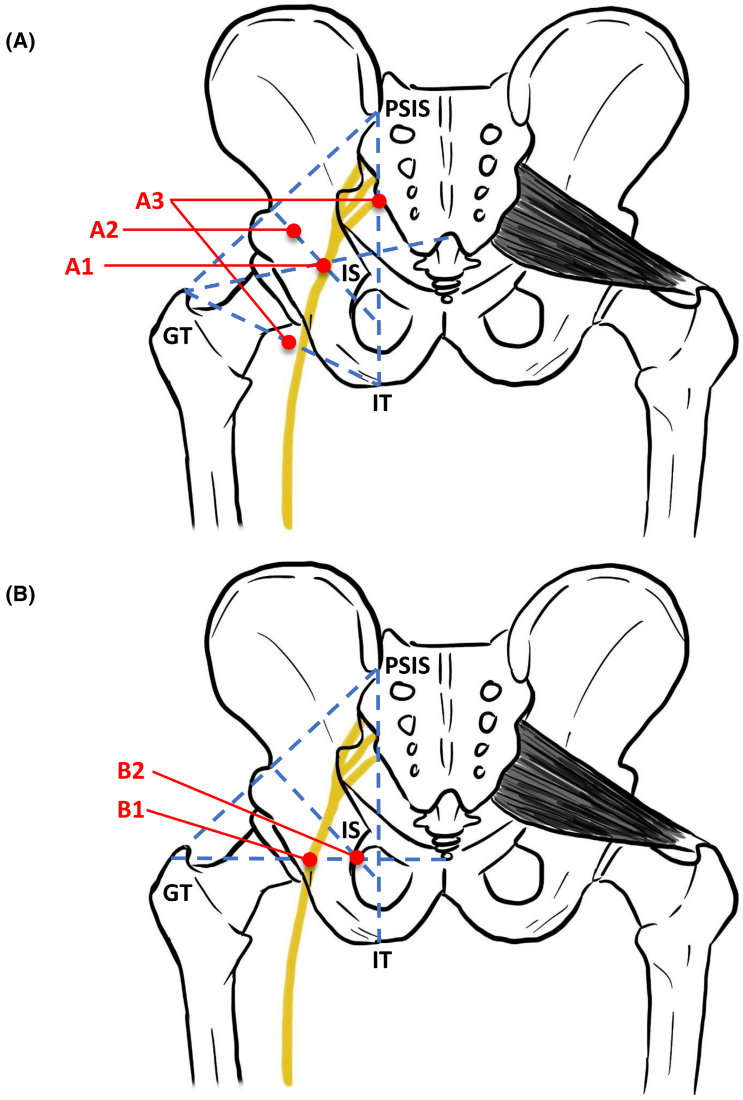

FIGURE 1 Illustration comparing the reported puncture sites for the posterior approach of sciatic nerve blockade in adult (A) and pediatric (B) literature. GT, greater trochanter; IS, ischial spine; IT, ischial tuberosity; PSIS, posterior superior iliac spine; SN, sciatic nerve. The yellow line represents the course of the sciatic nerve in the gluteal region.

	References (research study)	Description of landmarks to isolate SN
	ADULT	
A1	Miller, 2000; De Benedetto et al., 2001 (prospective randomized comparison study); Fournier et al., 2005 (retrospective study)	Intersection of line from GT to sacral hiatus with perpendicular line that bisects a line from PSIS to midpoint of GT
A2	Taboada et al., 2004 (prospective randomized comparison study)	4cm inferior to midpoint of a line joining PSIS and midpoint of GT
A3	Currin et al., 2015 (imaging study)	Point about 1/3 of the way along a line between PSIS and IT, curving laterally and inferiorly to a point midway between GT and IT
	PEDIATRIC	
B1	Dalens et al., 1990 (prospective randomized comparison study); Miller, 2000; Dalens, 2003; Acar et al., 2017 (cadaveric study)	Midpoint of line extending from tip of coccyx to GT
B2	Polaner et al., 2009	Point at which perpendicular line from midpoint of line from PSIS to GT intersects another line from GT to tip of coccyx

2.3 | Statistical analysis

All data were recorded in Microsoft Excel (version 16.0; 2019; Microsoft Corp.) and statistically analyzed using the RStudio (version 1.2.5033; 2019; RStudio, Inc.). Descriptive statistical analysis was calculated for the total sample, for each age group and for sex and side categories. The sciatic nerve and anatomical landmark distances were tested for normality using the Kolmogorov–Smirnov test. Pearson's or Spearman's rank correlation coefficient tests, as applicable, were used to determine the relationship between the morphometric parameters. A linear regression analysis was used to evaluate the relationship between age and the relevant

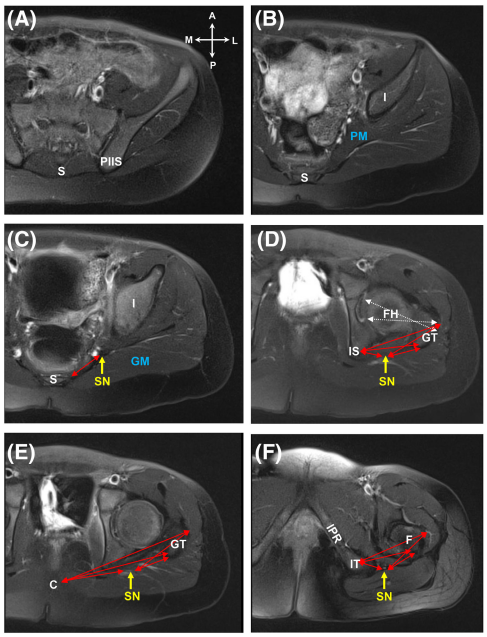

	Reference level	Parameter	Distance description
A	Level before sacroiliac joint disappears		
B	Level where SN appears anterior to PM within the greater sciatic foramen		
C	Level where SN appears posterior to PM and anterior to GM	SN-S	Midpoint of SN to most lateral point of S
D	Level before IS disappears	F1	Horizontal width from FH to most lateral GT (stature)
		F2	Diagonal width from FH to most lateral GT (stature)
		IS-F1	IS to most lateral point of GT
		IS-F2	IS to most medial point of GT
		SN-IS	IS to midpoint of SN
		SN-F3	Midpoint of SN to most lateral point of GT
		SN-F4	Midpoint of SN to most medial point of GT
E	Level before tip of coccyx disappears	C-F1	Tip of coccyx to most lateral point of GT
		C-F2	Tip of coccyx to most medial point of GT
		SN-C	Tip of coccyx to midpoint of SN
		SN-F1	Midpoint of SN to most lateral point of GT
		SN-F2	Midpoint of SN to most medial point of GT
F	Level of IT where IPR first appears	IT-F1	Midpoint of IT to most lateral point of F
		IT-F2	Midpoint of IT to most medial point of F
		SN-IT	Midpoint of IT to midpoint of SN
		SN-F5	Midpoint of SN to most lateral point of F
		SN-F6	Midpoint of SN to most medial point of F

FIGURE 2 MRI scans (axial view) of the left hip demonstrating the reference levels (A–F) and morphometric measurements taken of the sciatic nerve and anatomical landmarks. C, coccyx; F, femur; FH, femoral head; GM, gluteus maximus; GT, greater trochanter; I, ilium; IPR, inferior pubic ramus, IS, ischial spine; IT, ischial tuberosity; S, sacrum, SN, sciatic nerve; PIIS, posterior inferior iliac spine; PM, piriformis muscle. Orientation coordinate marker: A, anterior; L, lateral; M, medial; P, posterior.

morphometric parameters. Differences between sexes and sides of each age group were determined using the independent-samples *t* test or Wilcoxon signed rank test, depending on the normality assumption. Significance was determined at $p < 0.05$.

3 | RESULTS

3.1 | Descriptive statistics across age

The descriptive statistics for sciatic nerve morphometric parameters for the different age groups are summarized in Appendix 1. Overall, all morphometric parameters increased with the age of the patients.

3.2 | Sciatic nerve location relative to anatomical landmarks

The course of the sciatic nerve at different reference levels (A–F) relative to bony landmarks is illustrated in Figure 3.

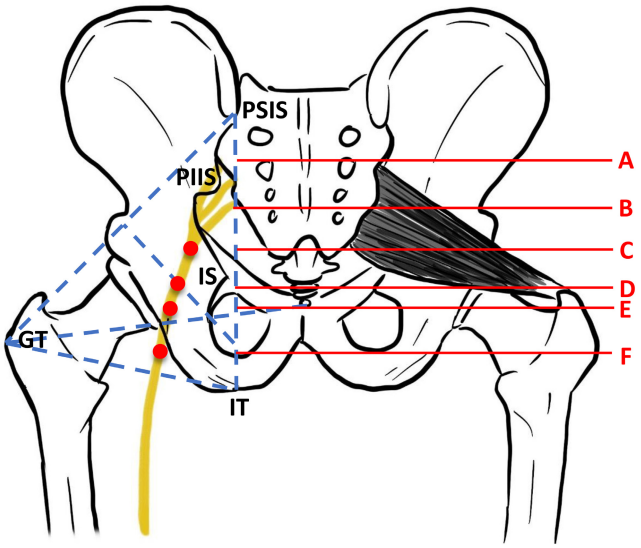

FIGURE 3 Illustration showing the course of the sciatic nerve at different reference levels (A–F). GT, greater trochanter; IS, ischial spine; IT, ischial tuberosity; PIIS, posterior inferior iliac spine; PSIS, posterior superior iliac spine. The yellow line represents the course of the sciatic nerve in the gluteal region.

3.3 | Correlation of morphometric parameters and regression with age

Most of the parameters strongly correlated with each other except for SN-S, SN-IS, SN-IT, and SN-F6 parameters (Figure 2). The strongest correlations ($r \geq 0.75$, $p < 0.001$) of morphometric parameters are summarized in Appendix 2. The linear regression correlation between patient age and morphometric parameters, including the distances between the femoral head and the greater trochanter measured for stature variation (F1 and F2 parameters), are illustrated in Figure 4. As expressed in Figure 4, the linear regression equations were executed for each of the variables as formulae for predicting the location of the sciatic nerve from bony landmarks using patient age.

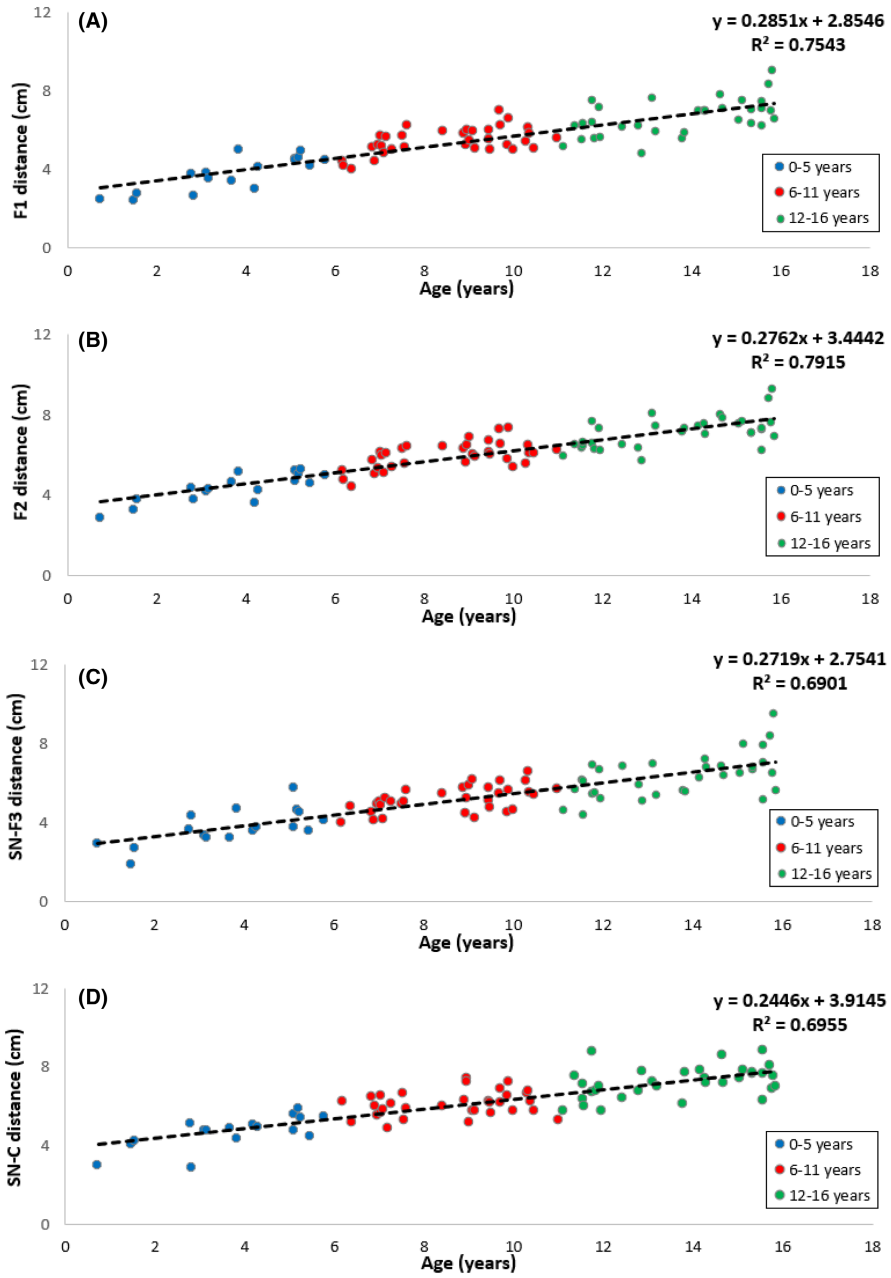

FIGURE 4 Scatter plots showing strong linear regressions between age of patient and parameters: F1 (A), F2 (B), SN-F3 (C), and SN-C (D). C, coccyx; F, femur; F1, horizontal distance from femoral head to most lateral point of greater trochanter; F2, diagonal distance from femoral head to most lateral point of greater trochanter; SN, sciatic nerve; SN-F3, distance from sciatic nerve to most lateral point of greater trochanter; SN-C, distance from sciatic nerve to tip of coccyx.

3.4 | Comparison of morphometric parameters between sexes and sides

When comparing sexes and sides across the different age groups, several strong evidence for differences were found between the morphometric parameters (Table 1). Between sexes, distances from the sciatic nerve to the lateral sacrum (SN-S), the most medial point of the greater trochanter at the level of coccyx (SN-F2) and ischial tuberosity (SN-F6) were different between the male and female groups. SN-S ($p = 0.023$) differed in the 6–11 years age group and SN-S ($p = 0.001$) and SN-F6 ($p = 0.029$) in the 12–16 years age group (Table 1). Between the left and the right sides of the hip, the following parameters showed strong evidence for differences: IS-F1 ($p = 0.020$), IS-F2 ($p = 0.027$), SN-F3 ($p = 0.014$), SN-F4 ($p = 0.027$), C-F1 ($p = 0.027$), SN-F1 ($p = 0.010$), and SN-F2 ($p = 0.010$). All these differences were found in the 0–5 years age group (Table 1).

3.5 | Sciatic nerve variation in the gluteal region

In one of the 84 MRI scans (6–11 years age group), the sciatic nerve bifurcated into its two distinct branches, common fibular and tibial nerves, at the level of the ischial tuberosity and inferior pubic ramus (reference level F) (Figure 5).

4 | DISCUSSION

This study examined the relationship between the sciatic nerve and the surrounding anatomical landmarks to determine the best predictable location of the sciatic nerve in the pediatric gluteal region. This is mapped and summarized visually in Figure 3. Several bony landmarks, including the greater trochanter of the femur,

TABLE 1 Comparison of statistically significant morphometric parameters between sexes and sides across age [Mean ± SD (Range) (cm)]

Parameter[a]	0–5 years ($n = 17$)		6–11 years ($n = 33$)		12–16 years ($n = 34$)	
SN-S	Male ($n = 6$)	Female ($n = 11$)	Male ($n = 20$)	Female ($n = 13$)	Male ($n = 16$)	Female ($n = 17$)
	1.87 ± 0.58 (1.02–2.45)	2.03 ± 0.38 (1.46–2.76)	2.43 ± 0.43 (1.68–3.20)	2.38 ± 0.40 (1.87–2.99)	3.08 ± 0.75[b] (1.95–4.43)	4.15 ± 0.88[b] (2.26–5.15)
IS-F1	Right ($n = 3$)	Left ($n = 14$)	Right ($n = 10$)	Left ($n = 23$)	Right ($n = 14$)	Left ($n = 19$)
	4.04 ± 0.57[b] (3.46–4.60)	5.38 ± 0.70[b] (3.59–6.22)	7.29 ± 0.54 (6.36–8.05)	7.20 ± 1.01 (5.50–9.47)	8.94 ± 1.54 (6.81–12.27)	8.78 ± 0.94 (6.93–10.48)
IS-F2	Right ($n = 3$)	Left ($n = 14$)	Right ($n = 10$)	Left ($n = 23$)	Right ($n = 14$)	Left ($n = 19$)
	2.21 ± 0.40[b] (1.79–2.58)	3.45 ± 078[b] (1.94–4.57)	4.79 ± 0.60 (4.22–6.22)	5.14 ± 0.92 (3.47–7.30)	6.30 ± 1.19 (4.85–8.61)	6.21 ± 0.94 (4.47–7.80)
SN-F3	Right ($n = 3$)	Left ($n = 14$)	Right ($n = 10$)	Left ($n = 23$)	Right ($n = 14$)	Left ($n = 19$)
	2.58 ± 0.65[b] (1.89–3.19)	4.00 ± 0.74[b] (2.93–5.77)	5.20 ± 0.53 (4.22–5.81)	5.18 ± 0.71 (3.95–6.59)	6.60 ± 1.40 (4.60–9.51)	6.22 ± 0.80 (4.40–7.26)
SN-F4	Right ($n = 3$)	Left ($n = 14$)	Right ($n = 10$)	Left ($n = 23$)	Right ($n = 14$)	Left ($n = 19$)
	0.89 ± 0.38[b] (0.52–1.28)	2.01 ± 0.92[b] (0.98–4.12)	2.66 ± 0.53 (1.94–3.61)	2.93 ± 0.72 (1.73–4.27)	3.82 ± 1.11 (2.12–5.67)	3.56 ± 0.85 (1.90–4.94)
C-F1	Right ($n = 3$)	Left ($n = 14$)	Right ($n = 10$)	Left ($n = 23$)	Right ($n = 14$)	Left ($n = 19$)
	6.85 ± 0.70[b] (6.08–7.46)	8.63 ± 1.13[b] (5.68–10.18)	11.17 ± 0.67 (10.10–12.26)	11.16 ± 1.11 (9.17–12.86)	13.67 ± 1.85 (10.13–17.05)	13.38 ± 1.27 (11.00–15.58)
SN-F1	Right ($n = 3$)	Left ($n = 14$)	Right ($n = 10$)	Left ($n = 23$)	Right ($n = 14$)	Left ($n = 19$)
	2.61 ± 0.41[b] (2.14–2.91)	4.03 ± 0.71[b] (2.98–5.32)	5.31 ± 0.58 (4.39–6.04)	5.21 ± 0.85 (3.70–6.59)	6.63 ± 1.39 (4.62–9.57)	6.24 ± 0.83 (4.53–7.56)
SN-F2	Male ($n = 6$)	Female ($n = 11$)	Male ($n = 20$)	Female ($n = 13$)	Male ($n = 16$)	Female ($n = 17$)
	1.53 ± 0.68 (0.71–2.29)	1.84 ± 0.99 (0.52–3.55)	2.50 ± 0.74[b] (1.41–4.11)	3.16 ± 0.80[b] (1.24–4.12)	3.57 ± 1.17 (2.00–5.65)	3.68 ± 0.87 (1.88–5.42)
SN-F2	Right ($n = 3$)	Left ($n = 14$)	Right ($n = 10$)	Left ($n = 23$)	Right ($n = 14$)	Left ($n = 19$)
	0.83 ± 0.27[b] (0.52–1.03)	1.92 ± 0.85[b] (0.71–3.55)	2.65 ± 0.58 (1.88–3.76)	2.84 ± 0.91 (1.24–4.12)	3.83 ± 1.20 (2.17–5.65)	3.48 ± 0.85 (1.88–5.07)
SN-F6	Male ($n = 6$)	Female ($n = 11$)	Male ($n = 20$)	Female ($n = 13$)	Male ($n = 16$)	Female ($n = 17$)
	1.29 ± 0.57 (0.71–2.38)	1.19 ± 0.34 (0.54–1.66)	1.90 ± 0.42 (1.24–2.78)	1.92 ± 0.39 (1.28–2.55)	2.30 ± 0.70[b] (1.26–3.62)	1.78 ± 0.52[b] (1.10–2.74)

Note: Shades highlighting significant parameters between sexes (green) and sides (blue).

Abbreviations: C, coccyx; F, femur; IS, ischial spine; S, sacrum, SN, sciatic nerve.

[a]see Figure 2 for parameter description.

[b]statistically significant ($p < 0.05$).

ischial spine, and ischial tuberosity of the hip bone and the tip of coccyx were identified and measured as relevant relative distances from the sciatic nerve, on axial plane MRI scans (Figure 2). An earlier cadaveric study verified the use of the greater trochanter and tip of coccyx as suitable landmarks for identifying the sciatic nerve in children.[12] Their sample, however, was restricted to a very small age group (less than 28 days old) and weight range (2.5–4.2 kg). The results of this study corroborate the use of the greater trochanter, tip of coccyx, ischial spine, and the ischial tuberosity as appropriate landmarks for identifying the sciatic nerve. In this study, depending on the individual, the ischial spine (reference level D) could appear slightly before or after the tip of coccyx (reference level E) on MRI (Figure 3). In young, non-weight bearing children, the coccyx is a palpable structure[12] and thus can be used as a more easily identifiable and reliable landmark during anesthetic blockades of the sciatic nerve.

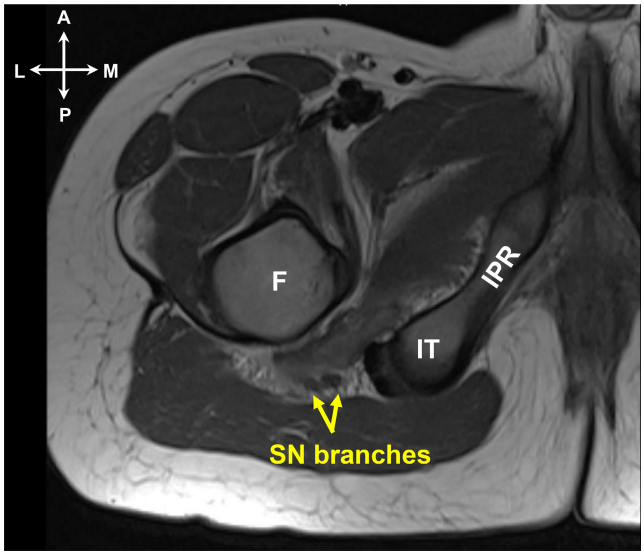

FIGURE 5 MRI scan (axial view) of the right hip showing sciatic nerve bifurcation at the level of ischial tuberosity and inferior pubic ramus at reference level F. F, femur; IPR, inferior pubic ramus, IT, ischial tuberosity; SN, sciatic nerve. Orientation coordinate marker: A, anterior; M, medial; P, posterior; L, lateral.

Based on our illustration demonstrating the location and course of the sciatic nerve relative to the bony landmarks (Figure 3), the sciatic nerve could be described as being approximately at the midpoint of a perpendicular line that bisects a line from the posterior superior iliac spine and greater trochanter, at the midpoint of a line extending from the tip of coccyx and greater trochanter, and at the midpoint of a line extending from the ischial tuberosity and greater trochanter. The resulting description agrees with past pediatric[1,4,12] and adult[10] studies (Figure 1). As the earlier imaging study suggested, the sciatic nerve curves laterally and inferiorly to a point midway between the ischial tuberosity and the greater trochanter.[10] They also reported mean distances of 6.4 cm between the sciatic nerve and the greater trochanter, and 5.7 cm between the sciatic nerve and the ischial tuberosity from their adult sample ($n = 100$). In neonatal cadavers ($n = 40$), the sciatic nerve was 1.2 cm medial to the greater trochanter and 1.5 cm lateral to the tip of coccyx.[12]

Most of the distances between the sciatic nerve and bony landmarks showed significant and strong positive correlation with growth and stature of the pediatric sample. The morphometric parameters correlated strongly with each other except for the SN-S and SN-F6 parameters. SN-S was taken at the level of sciatic nerve appearing between the piriformis and the gluteus maximus muscles, and both the nerve and sacrum were hard to visualize at this level due to the presence of the gluteal vessels and tendons of smaller lateral rotator muscles. SN-F6 was the distance between the sciatic nerve and the most medial point of femur at the level of the ischial tuberosity, and at this level, the most medial part of the femur was in some cases the lesser trochanter. This may explain the variability and weak correlations of SN-S and SN-F6 parameters.

Several strong linear regressions were found between the parameters and pediatric age and formulae using patient age were created to help predict the location of the sciatic nerve in the pediatric gluteal region (Figure 4). At the level of the ischial spine, the equation to determine the sciatic nerve location from the most lateral (i.e., palpable) point of the greater trochanter was:

"y (cm) = 0.2719 × Age (years) + 2.7541."

At the level of the coccyx, the formula to calculate the sciatic nerve distance from the tip of coccyx was:

"y (cm) = 0.2446 × Age (years) + 3.9145."

Such age-related formulae have implications for clinical guidelines involving the identification of the sciatic nerve in the pediatric gluteal region, particularly where ultrasound imaging and clinical expertise may be not available.

Stature is a measure independent of age and accommodates differences in sexes as well as in population groups. Stature estimated from the distance between the femoral head and the most lateral point of the greater trochanter (F1 and F2 parameters), correlated strongly with other morphometric parameters and the age of our pediatric sample ($n = 84$). F1 and F2 parameters strongly associated with sciatic nerve distances to medial and lateral points of the greater trocahnter and the tip of the coccyx ($r > 0.75$, $p = 0.001$). With age, F1 and F2 parameters showed strongest linear regressions ($R^2 = 0.754$ and 0.792, respectively; Figure 4), altogether suggesting that the location of the sciatic nerve could vary positively with age and growth (in height) of children. This was an expected finding, as it correlates well with our previous study on the pediatric knee region, which demonstrated age-related morphometric changes of the femoral bicondylar width and of the sciatic nerve and its branches relative to their surrounding anatomical structures in the popliteal region.[14]

When comparing sexes of each age groups, strong evidence for clinically significant differences was found (Table 1). The SN distances to sacrum (SN-S) and the most medial point of the greater trochanter at the level of coccyx (SN-F2) were longer in females, in 12–16 years and 6–11 years age groups, respectively. The sciatic nerve distance to the medial part of the greater trochanter at the level of the ischial tuberosity (SN-F6) was longer in the 12–16 years male group. The differences may be explained by the sexual dimorphism in the size and shape of the lower limb bones,[23,24] or could be due to the inconsistencies of SN-S and SN-F6 distance measurements as mentioned previously.

Further evidence for differences between the right and the left sides of the hip were also examined, only in the youngest (0–5 years) age group. The sciatic nerve distances to the greater trochanter (SN-F3, SN-F4, SN-F1, and SN-F2) and distances between landmarks (IS-F1, IS-F2, and C-F1) were all longer on the left side. This may be due to the fact that the right-side scans were taken of younger patients with average age of 2.2 years, as compared with the left-side scans taken of patients with average age of 4.1 years. Also, due to the much smaller sample size of right-side scans ($n = 3$), further study using larger and equal samples is required to confirm if the differences are truly laterality-based.

In one of the MRI scans observed, there was a bifurcation of the sciatic nerve at the level of the ischial tuberosity and the inferior

pubic ramus (reference level F) (Figure 5). This would correspond to the subgluteal region, just below the piriformis muscle. In our previous study of the pediatric knee, the average sciatic nerve bifurcation level for children aged 1–16 years was 3.2 cm above the level of femoral condyles.[14] Having a sciatic nerve bifurcating into its two branches above the mid-thigh region, is an anatomical variability, and needs to be considered clinically as this may have influence on procedures such as the subgluteal[9] or mid-thigh[25] approaches of the sciatic nerve blockade.

There are several limitations to this retrospective study, including the small sample size for the younger age groups. This was due to most of the available datasets for patients aged less than 2 years being Fast Low Angle Shot (FLASH) MRI scans, which are rapid scans with shortened measuring time but lessened image quality. Distorted or unclear images were also due to the limbs not being completely straightened or not taken in perfect symmetry, which could be a common challenge for infant patients. Future investigations using a larger sample size would also help to better inform the possible anatomical variations that may have clinical implications in regional anesthesia. The study also used two-dimensional axial planes to measure straight distances. Future studies can employ three-dimensional volume rendered reconstruction of the pediatric hip to better assess morphology and angular dimensions. As current literature suggests, prospective investigations using ultrasonography may verify our results and bring to light more informed ultrasound-guided techniques for the pediatric patients undergoing crucial lower limb surgeries and anesthetic procedures.[15,18]

5 | CONCLUSION

In summary, the anatomic relationship of the sciatic nerve relative to its surrounding bony landmarks of the pediatric hip varies linearly with increasing age, and distances from those landmarks can be predicted using linear regression, irrespective of differences in stature and subcutaneous fat. When visually mapping the variation and course of the sciatic nerve, the nerve lies at the midpoint of a line extending from the greater trochanter to coccyx and at the midpoint of a line from the greater trochanter to ischial tuberosity. Despite the limitations of having small sample size of younger age groups, this study is the first to provide a guideline for locating the sciatic nerve in the pediatric gluteal region, which may be used when ultrasound is not available or cannot be utilized due to poor resolution image, or as a confirmatory starting measurement to determine the expected location of the nerve prior to using the ultrasound.

ACKNOWLEDGMENT

None. Open access publishing facilitated by University of New South Wales, as part of the Wiley - University of New South Wales agreement via the Council of Australian University Librarians. Open access publishing facilitated by University of New South Wales, as part of the Wiley - University of New South Wales agreement via the Council of Australian University Librarians.

FUNDING INFORMATION

This research was carried out without external funding.

CONFLICT OF INTEREST

This research has no conflicts of interest declared.

DATA AVAILABILITY STATEMENT

The data that supports the findings of this study are available in the supplementary material of this article.

ORCID

Sarang Byun https://orcid.org/0000-0002-2455-9752
Nalini Pather https://orcid.org/0000-0001-5288-7713

REFERENCES

1. Dalens B. Lower extremity nerve blocks in pediatric patients. *Tech Reg Anesth Pain Manag*. 2003;7:32-47.
2. Bernière J, Schrayer S, Piana F, Vialle R, Murat I. A new formula of age-related anatomical landmarks for blockade of the sciatic nerve in the popliteal fossa in children using the posterior approach. *Pediatr Anesth*. 2008;18:602-605.
3. Kang C, Hwang D-S, Song J-H, et al. Clinical analyses of ultrasound-guided nerve block in lower-extremity surgery: a retrospective study. *J Orthop Surg*. 2021;29:1-9.
4. Dalens B, Tanguy A, Vanneuville G. Sciatic nerve blocks in children: comparison o fthe posterior, anterior and lateral approaches in 180 pediatric patients. *Anesth Analg*. 1990;70:131-137.
5. Taboada M, Rodríguez J, ALvarez J, Cortés J, Gude F, Atanassoff PG. Sciatic nerve block via posterior labat approach is more efficient than lateral popliteal approach using a double-injection technique. *Anesthesiology*. 2004;101:138-142.
6. Fournier R, Weber A, Gamulin Z. Posterior labat vs. lateral popliteal sciatic block: posterior sciatic block has quicker onset and shorter duration of anaesthesia. *Acta Anaesthesiol Scand*. 2005;49:683-686.
7. Salinas FV. Evidence basis for ultrasound guidance for lower-extremity peripheral nerve block: update 2016. *Reg Anesth Pain Med*. 2016;41:261-274.
8. Miller RD. *Anesthesia*. Vol 1. 5th ed. Churchill Livingstone; 2000.
9. De Benedetto P, Bertini L, Casati A, et al. A new posterior approach to the sciatic nerve block: a prospective, randomized comparison with the classic posterior approach. *Anesth Analg*. 2001;93:1040-1044.
10. Currin SS, Mirjalili SA, Meikle G, Stringer MD. Revisiting the surface anatomy of the sciatic nerve in the gluteal region. *Clin Anat*. 2015;28:144-149.
11. Polaner DM, Suresh S, Coté CJ. Regional Anesthesia. *A Practice of Anesthesia for Infants and Children*. 4th ed. W.B Saunders; 2009:867-910.
12. Acar AA, Bösenberg AT, van Schoor A-N. Anatomical description of the sciatic nerve block at the subgluteal region in a neonatal cadaver population. *Pediatr Anesth*. 2017;27:643-647.
13. Suresh S, Simion C, Wyers M, Swanson M, Jennings M, Iyer A. Anatomical location of the bifurcation of the sciatic nerve in the posterior thigh in infants and children: a formula derived from MRI imaging for nerve localization. *Reg Anesth Pain Med*. 2007;32:351-353.
14. Byun S, Gordon J, Morris S, Jacob T, Pather N. A computed tomography and magnetic resonance imaging study of the variations of the sciatic nerve branches of the pediatric knee: Implications for peripheral nerve blockade. *Clin Anat*. 2019;32:836-850.

15. Marhofer P, Harrop-Griffiths W, Willschke H, Kirchmair L. Fifteen years of ultrasound guidance in regional anaesthesia: Part 2—recent developments in block techniques. *Br J Anaesth*. 2010;104:673-683.
16. Oberndorfer U, Marhofer P, Bösenberg A, et al. Ultrasonographic guidance for sciatic and femoral nerve blocks in children. *Br J Anaesth*. 2007;98:797-801.
17. Tsui BCH, Suresh S. Ultrasound imaging for regional anesthesia in infants, children, and adolescents: a review of current literature and its application in the practice of extremity and trunk blocks. *Anesthesiology*. 2010;112:473-492.
18. Delvi M. Ultrasound-guided peripheral and truncal blocks in pediatric patients. *Saudi J Anaesth*. 2011;5:208-216.
19. Bosenberg A. Regional anesthesia in children: the future. *Pediatr Anesth*. 2012;22:564-569.
20. Donovan AD, Nicholls BJ. Ultrasound in anaesthesia; the best kept secret. *Ultrasound*. 2008;16:24-27.
21. Sala-Blanch X, Carrera A, Hurtado P. Anatomy–ultrasound correlation for selected peripheral nerve blocks. *Tech Reg Anesth Pain Manag*. 2008;12:146-152.
22. Brasher C, Gafsous B, Dugue S, et al. Postoperative pain management in children and infants: an update. *Paediatr Drugs*. 2014;16:129-140.
23. Arsuaga JL, Carretero JM. Multivariate analysis of the sexual dimorphism of the hip bone in a modern human population and in early hominids. *Am J Phys Anthropol*. 1994;93:241-257.
24. Fischer B, Mitteroecker P. Allometry and sexual dimorphism in the human pelvis. *Anat Rec*. 2017;300:698-705.
25. Barrington JM, Lai KS-L, Briggs AC, Ivanusic JJ, Gledhill SR. Ultrasound-guided midthigh sciatic nerve block—a clinical and anatomical study. *Reg Anesth Pain Med*. 2008;33:369-376.

How to cite this article: Byun S, Morris S, Pather N. Magnetic resonance imaging study of the sciatic nerve variation in the pediatric gluteal region: Implications for the posterior approach of the sciatic nerve blockade. *Pediatr Anesth*. 2022;32:1355-1364. doi:10.1111/pan.14545

APPENDIX 1 Descriptive summary of morphometric parameters across age [Mean ± SD (Range) (cm)]

Parameter[†]	0–5 years ($n = 17$)	6–11 years ($n = 33$)	12–16 year ($n = 34$)	Total ($n = 84$)
SN-S	1.98 ± 0.45 (1.02–2.76)	2.41 ± 0.41 (1.68–3.20)	3.63 ± 0.97 (1.95–5.15)	2.81 ± 0.98 (1.02–5.15)
F1	3.79 ± 0.87 (2.41–5.00)	5.45 ± 0.67 (3.97 ± −6.99)	6.65 ± 0.91 (4.82–9.07)	5.58 ± 1.33 (2.41–9.07)
F2	4.34 ± 0.72 (2.84–5.28)	5.95 ± 0.66 (4.39–7.32)	7.13 ± 0.79 (5.74–9.27)	6.09 ± 1.26 (2.84–9.27)
IS-F1	5.14 ± 0.84 (3.46–6.22)	7.23 ± 0.88 (5.50–9.47)	8.85 ± 1.21 (6.81–12.27)	7.45 ± 1.71 (3.46–12.27)
IS-F2	3.23 ± 0.87 (1.79–4.57)	5.03 ± 0.84 (3.47–7.30)	6.25 ± 1.03 (4.47–8.61)	5.15 ± 1.45 (1.79–8.61)
SN-IS	1.75 ± 0.24 (1.11–2.03)	2.35 ± 0.33 (1.8–3.51)	2.67 ± 0.44 (1.73–3.62)	2.35 ± 0.50 (1.11–3.62)
SN-F3	3.75 ± 0.90 (1.89–5.77)	5.19 ± 0.65 (3.95–6.59)	6.38 ± 1.09 (4.40–9.51)	5.37 ± 1.33 (1.89–9.51)
SN-F4	1.81 ± 0.95 (0.52–4.12)	2.85 ± 0.67 (1.73–4.27)	3.67 ± 0.96 (1.90–5.67)	2.96 ± 1.09 (0.52–5.67)
C-F1	8.31 ± 1.26 (5.68–10.18)	11.16 ± 0.99 (9.17–12.86)	13.50 ± 1.52 (10.13–17.05)	11.51 ± 2.31 (5.68–17.05)
C-F2	6.35 ± 1.26 (3.91–8.23)	8.82 ± 0.93 (6.85–10.83)	10.82 ± 1.38 (8.26–13.18)	9.11 ± 2.05 (3.91–13.18)
SN-C	4.7 ± 0.82 (2.92–5.94)	6.11 ± 0.62 (4.87–7.41)	7.23 ± 0.79 (5.82–8.84)	6.27 ± 1.19 (2.92–8.84)
SN-F1	3.78 ± 0.86 (2.14–5.32)	5.24 ± 0.77 (3.70–6.59)	6.40 ± 1.10 (4.53–9.57)	5.40 ± 1.35 (2.14–9.57)
SN-F2	1.7 ± 0.88 (0.52–3.55)	2.78 ± 0.82 (1.24–4.12)	3.63 ± 1.01 (1.88 ± 5.65)	2.90 ± 1.15 (0.52–5.65)
IT-F1	4.43 ± 0.7 (3.28–5.46)	6.23 ± 0.61 (4.59–7.52)	7.48 ± 1.07 (5.77–9.90)	6.38 ± 1.39 (3.28–9.90)
IT-F2	2.13 ± 0.35 (1.49–2.98)	3.13 ± 0.6 (1.66–4.52)	3.81 ± 0.99 (2.23–6.20)	3.21 ± 0.96 (1.49–6.20)
SN-IT	2.01 ± 0.36 (1.43–2.87)	2.52 ± 0.35 (2.00–3.13)	2.74 ± 0.39 (1.92–3.52)	2.51 ± 0.45 (1.43–3.52)
SN-F5	2.86 ± 0.59 (2.12–3.72)	4.12 ± 0.52 (3.17–5.12)	5.16 ± 0.97 (3.23–7.19)	4.29 ± 1.12 (2.12–7.19)
SN-F6	1.22 ± 0.42 (0.54–2.38)	1.91 ± 0.40 (1.24 ± −2.78)	2.03 ± 0.66 (1.10 ± 3.62)	1.83 ± 0.60 (0.54–3.62)

Abbreviations: C, coccyx; F, femur; IS, ischial spine; IT, ischial tuberosity; S, sacrum, SN, sciatic nerve.

[†]see Figure 2 for parameter description.

APPENDIX 2 Summary of strong correlations of morphometric parameters ($r \geq 0.75$, $p < 0.001$)

Parameter[†]	Correlated parameter	*r*-value
F1	F2	0.95
	IS-F1	0.91
	IS-F2	0.92
	SN-F3	0.88
	SN-F4	0.84
	C-F1	0.94
	C-F2	0.95
	SN-C	0.80
	SN-F1	0.89
	SN-F2	0.75
	IT-F1	0.89
	IT-F2	0.76
	SN-F5	0.85
F2	IS-F1	0.91
	IS-F2	0.86
	SN-F3	0.88
	SN-F4	0.77
	C-F1	0.93
	C-F2	0.91
	SN-C	0.79
	SN-F1	0.89
	IT-F1	0.87
	SN-F5	0.85
SN-S	C-F1	0.75
	C-F2	0.76
	IT-F1	0.75
IS-F1	IS-F2	0.94
	SN-F3	0.93
	SN-F4	0.82
	C-F1	0.94
	C-F2	0.92
	SN-C	0.78
	SN-F1	0.92
	IT-F1	0.89
	IT-F2	0.77
	SN-F5	0.87
IS-F2	SN-F3	0.89
	SN-F4	0.91
	C-F1	0.89
	C-F2	0.92
	SN-F1	0.89
	SN-F2	0.79
	IT-F1	0.91
	IT-F2	0.78
	SN-F5	0.89
SN-F3	SN-F4	0.91
	C-F1	0.92
	C-F2	0.89
	SN-F1	0.95
	SN-F2	0.78
	IT-F1	0.84
	SN-F5	0.85
SN-F4	C-F1	0.82
	C-F2	0.88
	SN-F1	0.89
	SN-F2	0.85
	IT-F1	0.82
	SN-F5	0.82
C-F1	C-F2	0.97
	SN-C	0.89
	SN-F1	0.89
	IT-F1	0.88
	IT-F2	0.77
	SN-F5	0.85
C-F2	SN-C	0.86
	SN-F1	0.89
	SN-F2	0.78
	IT-F1	0.90
	IT-F2	0.79
	SN-F5	0.86
SN-C	IT-F1	0.76
SN-F1	SN-F2	0.85
	IT-F1	0.86
	IT-F2	0.76
	SN-F5	0.85
IT-F1	IT-F2	0.88
	SN-F5	0.95
IT-F2	SN-F5	0.80

Abbreviations: C, coccyx; F, femur; IS, ischial spine; IT, ischial tuberosity; S, sacrum, SN, sciatic nerve.

[†]see Figure 2 for parameter description.